

<https://doi.org/10.52676/1729-7885-2022-4-63-73>
УДК 534.222.2

SYNTHESIS OF DIFFERENT METAL DOPED ZnAl-LDH/PVA NANOCOMPOSITES FOR ADSORPTION AND PHOTOCATALYTIC APPLICATIONS

O.O. Balayeva

Baku State University, Baku, Azerbaijan

E-mail for contacts: oobalayeva@gmail.com; ofeliyabalayeva@bsu.edu.az

Due to their high surface area, electronic properties, energy storage performance and catalytic activity, two-dimensional (2D) nanostructures have attracted significant interest and great attention in developing science. Layered double hydroxides (LDHs) belong to 2D nanostructures and have a high surface area, very important physicochemical properties, and biological activity. However, there has always been great interest in their doping to enhance and improve these unique properties, especially photocatalytic activity. In this work, ZnAl-based LDHs were synthesized and their doping with active- (Ca, Sr), transition- (Co, Cu, Cd, Ni, Pb, Fe), noble- (Ag) and rare earth- (La) metals were carried out by impregnation method. The removal of cationic and anionic dyes from aqueous solutions by adsorption and photodegradation on as-synthesized and doped ZnAl-LDH/PVA nanocomposite was also studied. The obtained results were correlated with the structure and physicochemical properties of the nanocomposites.

Keywords: *Layered Double Hydroxides (LDH); metal-doped, sorption; photodegradation; Rhodamine 6G; Ponceau 4R.*

1. INTRODUCTION

2D nanomaterials are generally layered materials can be classified according to their chemical composition, properties, and application. They are classified based on different criteria like sheets layered nanostructures, films, nano-patterned surfaces, and coatings [1]. Graphene [2, 3], graphene oxide (GO) [4], Mxenes [5], silicate clays [6], hydroxides, and layered double hydroxides (LDHs) [7], [8], some of transition metal chalcogenides [9–11], some of transition metal oxides (TMOs) or mixed metal oxide (MMO) [12, 13], black phosphorus nanosheets (BPN), Boron and boron nitride nanosheet, antimonene (AM) and antimonene oxide nanosheet [14] are sheet-like layered nanostructures possess excellent physical, mechanical, chemical and biochemical properties due to structures, high surface area and surface charge. In order to obtain new physicochemical properties in nanomaterials, new 2D nanomaterials are currently being synthesized in science, or modification of known nanostructures is being carried out. In layered nanostructures, atoms on the layer chemically bonded each other and there are physical interactions between the layers to form bulk crystals [1], [15, 16].

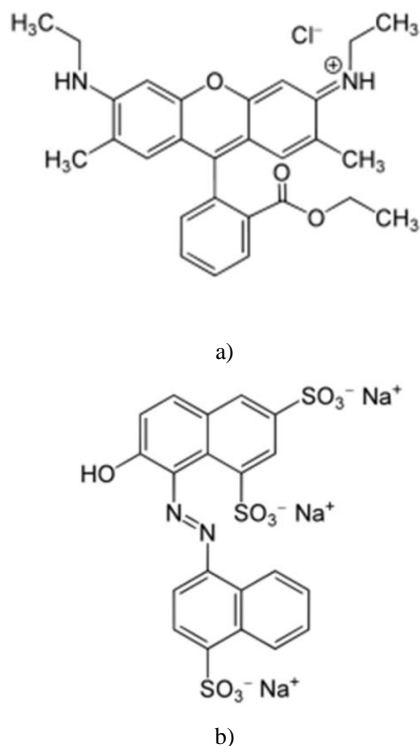
This research article will focus on layered double hydroxides (LDHs) which are very important representatives of 2D nanostructures containing positively charged layers and their compositional properties will be discussed in detail. LDHs are layered crystalline hydroxides with excellent conductivity, surface active, optical, electrical, mechanical, thermal, magnetic, catalytically properties which have broad application in photocatalysis [17–19] supercapacitors [20, 21], fire retardant [22, 23], energy storage [24, 25], anion exchange materials [26, 27], biomedicine [28, 29], electrochemical sensors [30], and other field. As known, to enhance or change the electrical, optical and structural properties of semiconductor nanoparticles, it is very important to include or

dope small or large amounts of other elements on their surface or inside. Many experiments on metal doping to TiO₂ have been carried out in the literature [31]. Depending on the nature and amount of the dopant and method, various but excellent results have been obtained [32]. However, since LDHs themselves are formed from atoms of various elements, their doping has not been widely studied. It is for this reason that by taking LDH with a uniform composition (ZnAl), it was doped by the method of impregnation with metals of different activity. The photocatalytic activity of doped materials was studied by decomposition of dye compounds under sun light and explained in detail.

2. EXPERIMENT

2.1. Synthesis of Zn Al LDH in PVA matrix

Zinc-aluminum layered double hydroxide (ZnAl LDH) nanoparticles in polyvinyl alcohol (PVA) matrix was synthesized via co-formation method [33]. 40 mL of 10% PVA solution was added into the mixed metal salt solution before the co-precipitation with Zn/Al = 3/1 molar ratio and mixed for 30 min. 25 mL of 5 M sodium hydroxide (NaOH) solution was drop wise added to the mixed salt solution. The pH of the sample was adjusted to ~10 by adding some additional drops of NaOH solution. The obtained slurry was aged for 2 weeks and heated at 90 °C for four days, washed with hot distilled water (~98°C), dried at room condition (at 25 °C), cuted into pieces and used for the adsorption and sunlight photodegradation of anionic and cationic dyes like Ponceau 4R (P4R) and Rhodamin 6G (R6G). The chemical structures of ponceau 4R and Rhodamin 6G are shown at Scheme 1:



Scheme 1. The molecular structure of Rhodamine 6G (a) and Ponceau 4R (b)

2.2. Doping of Zn Al LDH by impregnation method

The metal doping [cobalt (Co), copper (Cu), cadmium (Cd), nickel (Ni), lead (Pb), iron (Fe), silver (Ag), lanthanum (La), calcium (Ca) and strontium (Sr)] of the obtained nanocomposite was carried out for enhancing the photodegradation. The pathway of nanocomposite synthesis can be shown as follow: zinc sulfate heptahydrate ($\text{ZnSO}_4 \times 7\text{H}_2\text{O}$) and aluminium sulfate octadecahydrate [$\text{Al}_2(\text{SO}_4)_3 \times 18\text{H}_2\text{O}$] water solutions were prepared \rightarrow mixed together (Zn/Al = 3:1) \rightarrow added into PVA solution \rightarrow titrated with 5 M NaOH \rightarrow adjusted to pH 10 \rightarrow strongly shaken \rightarrow heated at 90 °C \rightarrow washed \rightarrow dried.

The pathway of metal doping can be shown as follow: Well dried and cutted nanocomposite obtained as above was added into 1mM metal salt solutions of iron (II) sulfate heptahydrate ($\text{FeSO}_4 \times 7\text{H}_2\text{O}$), nickel(II) nitrate hexahydrate [$\text{Ni}(\text{NO}_3)_2 \times 6\text{H}_2\text{O}$], cobalt (II) nitrate hexahydrate [$\text{Co}(\text{NO}_3)_2 \times 6\text{H}_2\text{O}$], lead (II) nitrate (PbNO_3), cadmium nitrate tetrahydrate [$\text{Cd}(\text{NO}_3)_2 \times 4\text{H}_2\text{O}$], copper sulfate pentahydrate ($\text{CuSO}_4 \times 5\text{H}_2\text{O}$), calcium nitrate (CaNO_3), strontium nitrate hexahydrate [$\text{Sr}(\text{NO}_3)_2 \times 6\text{H}_2\text{O}$] and silver nitrate (AgNO_3) \rightarrow aged for 4 h in a dark \rightarrow heated for 3h at 90°C \rightarrow cooled down till room temperature \rightarrow washed \rightarrow dried at room condition \rightarrow heated at 150°C for 7h \rightarrow used for the sorption and photodegradation.

Lanthanum (La) doped ZnAl-LDH was synthesized by mechanically mixing of as-precipitated LDH solution with lanthanum oxide 1% La_2O_3 .

2.3. An overview of the synthesis pathway of metal doped LDH

The choice of method for the synthesis of LDHs directly affects their crystallization. Sometimes, even if the method is the same, the crystallization may not go well if the reaction conditions and parameters are not chosen properly. For this, some scientists apply an aging for the synthesis.

Fe-doped LDH was synthesized as an effective photocatalyst for the Cr(VI) reduction of [34]. In the process, 1.19 g of $\text{Zn}(\text{NO}_3)_2 \times 6\text{H}_2\text{O}$ and 0.11 mL of TiCl_4 were added into 50 mL of deionized water \rightarrow added 1.5 g of urea \rightarrow mixed \rightarrow heated at 130 °C for 12 h \rightarrow followed by ultrasonication by adding montmorillonite in 10, 20 and 30 wt% for 3 h \rightarrow refluxed for 12 h \rightarrow filtrated \rightarrow washed with the DI water. For the Fe doping, the obtained precipitate (0.2 g) was dispersed in $\text{Fe}(\text{NO}_3)_3 \times 9\text{H}_2\text{O}$ solution (200 mL 0.015 mM) \rightarrow stirred for 10 min at pH 3 \rightarrow filtrated \rightarrow washed with deionized water \rightarrow dried at 75 °C for 24 h in an oven [34]. In another work, the synthesis of Fe-doped ZnAl-LDH, $\text{Zn}(\text{NO}_3)_2$ (6 mM) and a variable mixture of $\text{Al}(\text{NO}_3)_3$ and $\text{Fe}(\text{NO}_3)_3$ (2 mM) was added (1 mL/min) to the carbonate solution (pH 10) \rightarrow stirred at 50 °C for one hour \rightarrow pH adjusting to 10 with 1M KOH \rightarrow filtered \rightarrow dried at 100 °C for one hour [35]. In the synthesis of Ni-doped ZnAl-LDH, the composition of the precursor consisted of 2 mM $\text{Al}(\text{NO}_3)_3$ and 2 mM of a variable mixture of $\text{Zn}(\text{NO}_3)_2$ and $\text{Ni}(\text{NO}_3)_2$ solutions [35]. In the synthesis of Mn-doped Zn-Al LDHs with 0.5, 1, and 3.0% of Mn, the nitrate salts of Zn, Mn and Al in adequate proportion were dissolved in distilled water \rightarrow heated at 90 °C by hydrolysis with urea (NH_2CONH_2) \rightarrow pH was adjusted to 10 with $\text{NaHCO}_3/\text{NaOH}$ solution \rightarrow vigorously stirred at 90 °C \rightarrow refluxed during 36 h \rightarrow filtered \rightarrow washed with hot water (90 °C) \rightarrow dried at 100 °C for 12 h [36]. In the Cerium (Ce) doped LDH experiment, $\text{Zn}(\text{NO}_3)_2 \times 6\text{H}_2\text{O}$ (0.05 M), $\text{Al}(\text{NO}_3)_3 \times 9\text{H}_2\text{O}$ and $\text{Ce}(\text{NO}_3)_3 \times 6\text{H}_2\text{O}$ (together with 0.025 M) were dissolved boiled-distilled water (100 mL) \rightarrow added to 200 mL of NaNO_3 solution (0.1 M) under stirring at room temperature approximately 1.5 h \rightarrow adjusted pH = 10.0 by the addition of 2 M NaOH solution \rightarrow aged at 65 °C for 18 h \rightarrow filtered \rightarrow washed with boiled distilled water by three times \rightarrow dried at 60 °C [37]. In Terbium (Tb) doped ZnCr-LDH synthesis, two aqueous solutions (0.2 M Zn nitrate, 0.1 M Cr+Tb nitrates precursor and bases like 1M NaOH and 0.5 M Na_2CO_3) were prepared \rightarrow simultaneously added to deionized 100 mL of water \rightarrow the pH maintained at 9 \rightarrow transferred into an autoclave \rightarrow hydrothermally treated at 120 °C for 24 h \rightarrow filtered \rightarrow washed with deionized water \rightarrow dried at 60 °C for 24 h. 0.5% Tb^{3+} doped LDH shows high performance in oxygen evolution ($1022 \mu\text{mol}\cdot\text{h}^{-1}\cdot\text{g}^{-1}$) among other ratios [38]. In the experiment of synthesis of Dy doped LDH with a 30 : 9 : 1 ratio 4.4709 g of $\text{Zn}(\text{NO}_3)_2 \cdot 6\text{H}_2\text{O}$, 2.6671 g of $\text{Al}(\text{NO}_3)_3 \cdot 9\text{H}_2\text{O}$, and

0.2741 g of $\text{Dy}(\text{NO}_3)_3$ dissolved in 250 mL distilled water in nitrogen atmosphere \rightarrow titrated with 4% ammonia solution \rightarrow pH adjusted to 9 \rightarrow recovered the white powder \rightarrow washed with distilled water \rightarrow dried at 60 °C. In the experiment of Lanthanum (La) doped LDHs, $\text{Zn}(\text{NO}_3)_2 \times 6\text{H}_2\text{O}$ solution was mixed with $\text{Al}(\text{NO}_3)_3 \times 9\text{H}_2\text{O}$ and $\text{La}(\text{NO}_3)_3 \times 6\text{H}_2\text{O}$ mixed solution and dropwise added with together base solution containing NaOH and Na_2CO_3 \rightarrow stirred for 4 h at 85 °C at 10 pH \rightarrow aged for 20 h at 65 °C \rightarrow filtered \rightarrow washed \rightarrow dried and ground [39].

In another work, a mixed solution containing $\text{Zn}(\text{NO}_3)_2 \times 6\text{H}_2\text{O}$ (1.0 g), $\text{Cr}(\text{NO}_3)_3 \times 9\text{H}_2\text{O}$ (0.27 g) and $\text{La}(\text{NO}_3)_3 \times 6\text{H}_2\text{O}$ (0.2 g) and a mixed base solution containing 2 M NaOH and 0.5 M Na_2CO_3 were added to a 3-necked flask simultaneously \rightarrow pH was adjusted to 9–10 by adding 1 M NaOH \rightarrow stirring for 12 h \rightarrow transferred to Teflon-lined stainless steel autoclaves \rightarrow heated at 160 °C for 24 h \rightarrow centrifuged \rightarrow washed with deionized water \rightarrow dried at 80 °C in an oven for 6 h [40].

3. RESULTS AND DISCUSSION

3.1. Physical-chemical characterization of as-obtained ZnAl-LDH/PVA nanocomposite

XRD results of as-obtained and P4R adsorbed, photodegraded ZnAl-LDH/PVA nanocomposite are given in Figure 1. It is seen that the expected diffraction peaks of ZnAl-LDH with 003; 006; 101; 015; 018; 110 and 113 Miller index are observed which is confirm the formation of hydrotalcite-like (JCPDS No. 48–1023) structure. Because the P4R is an anionic dye, it is intercalated the layered structure. The basal spacing increased from 0.7 nm to 0.724 nm and 0.762 nm after the adsorption and photodegradation of P4R, respectively. The diffraction peak corresponding 003 Miller index doubles after the photodegradation which is explained by the formation of two phases (relaxed and strained) under the light [41]. The average particle size increased subsequently from 17 nm to 12 nm and 4 nm by the sorption and photodegradation, respectively. It is explained by the fact that, with the increase in the distance between the layers, the stability of the crystal lattice is weakened and the layers are expanded and separated. Since the R6G is a cationic dye, it could not intercalate the positive LDH layers and did not expand the interlayer distance. Therefore, there was no essential change in the XRD diffractogram after the sorption.

The FTIR spectra of as-obtained and P4R dye adsorbed ZnAl-LDH/PVA nanocomposite are shown in Figure 2. The transmittance bands fitting $-\text{OH}$ ($3600\text{--}3100\text{ cm}^{-1}$) of water, alcohol and carboxylic acid molecules were observed more clearly after the adsorption of anionic dye (P4R). It is related to the fact that some of the water molecules also entered between the

layers during the intercalation via dye adsorption. The band fitting to asymmetrical R-SO_3^- is observed after the sorption of P4R molecules. The plenty amount (3) of aryl sulfonate group on the dye molecule made the band significantly intensive. The bands observed at frequency 1651 cm^{-1} , 1558 cm^{-1} , 1492 cm^{-1} match up with H_2O , $-\text{N}=\text{N}-$, $-\text{C}=\text{C}-$, respectively [42]. Symmetrical $-\text{SO}_3^-$ falls at 1200 cm^{-1} and 1141 cm^{-1} frequency. The bands corresponding metal hydroxides (739 cm^{-1} for Al-O-H and 690 cm^{-1} for Zn-O-H (Figure 2, a) are shifted to high wavenumber (776 cm^{-1} for Al-O-H and 717 cm^{-1} for Zn-O-H (Figure 2, b) after the adsorption of P4R. It is explained by the fact that the interlayer physical interaction has weakened because of the intercalation. Therefore, the free energy of the hydroxide layer increased [43].

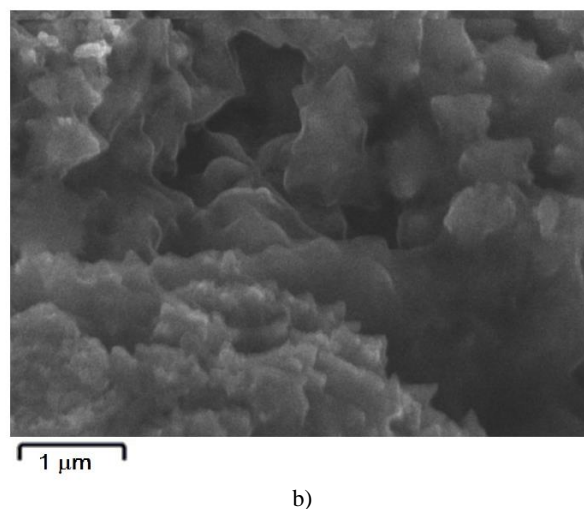
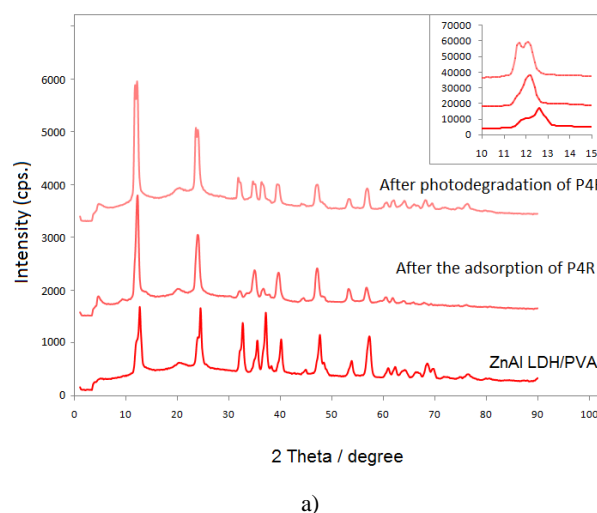


Figure 1. XRD pattern (A) and SEM image of ZnAl-LDH/PVA nanocomposite

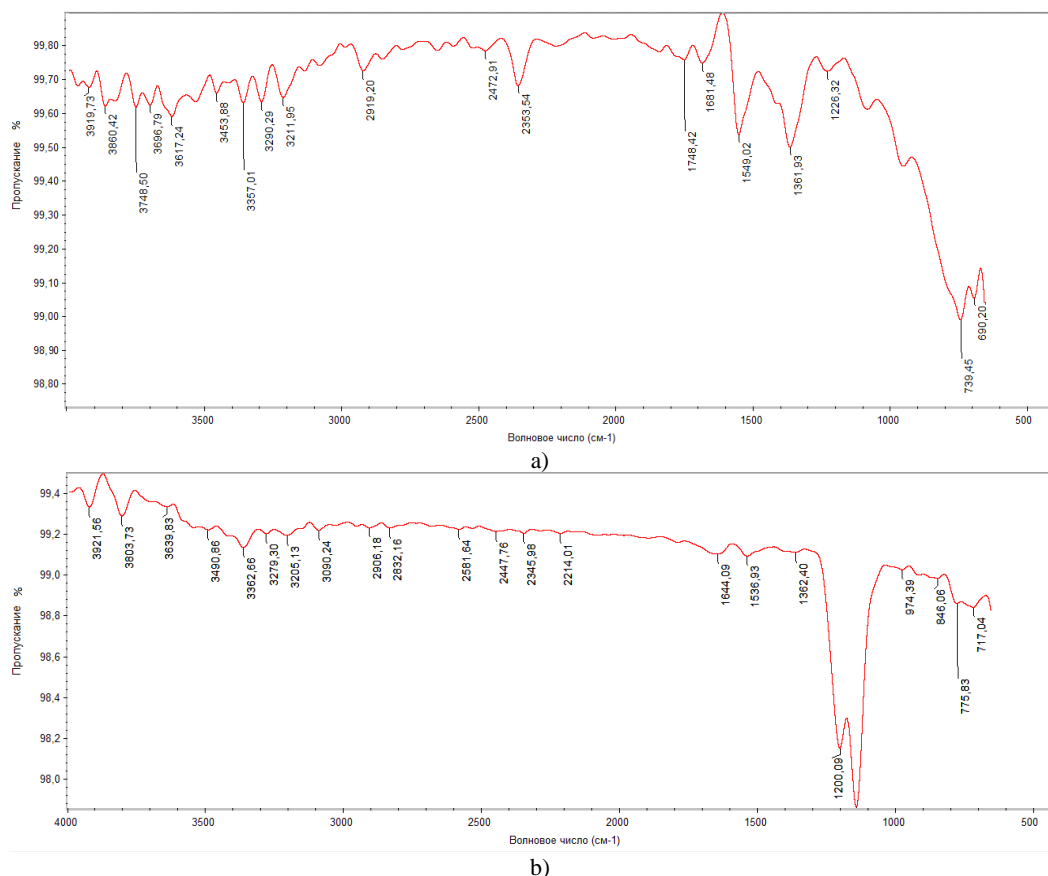


Figure 2. FTIR spectra of as-obtained (a) and P4R adsorbed (b) ZnAl-LDH/PVA nanocomposite

3.2. Adsorption and photodegradation of anionic (P4R) and cationic (R6G) dyes onto ZnAl-LDH/PVA nanocomposite

Sorption and photodegradation processes were taken place at a neutral pH of 5 ppm (R6G) and 20 ppm (P4R) of dye concentrations. 10 mg of sorbent in 10 mL of dye solution was taken, and the maximal absorbance was detected as 517 and 527 nm for P4R and R6G by Ultra-violet-visible (UV-Vis) spectrometer, respectively. As can be seen from table 1, the P4R sorption degree of undoped pure nanocomposite is low than metal doped ones. It is increased by Cd, Cu, Fe, Co, Ni and Ca dopants and decreased by Ag and Sr dopants. The increase of sorption degree by doped nanocomposites can be explained by the increase of positive charges of metals which enhanced the adsorption of anionic P4R dye by electrostatic effect onto positively charged nanocomposite. The decreasing of the sorption degree with Ag and Sr can be explained by the tendency of silver to sulphidation and strontium to oxidation in open air. Because silver shows +1 and +2 oxidation states it creates many defects in the LDH structure and it must increase the photocatalytic activity. But here the activity of Ag-doped LDH photocatalyst increased for the degradation of cationic dye (R6G), but not for anionic dye (P4R). It can be explained by the fact that the doping of metals was carried out by the impregnation method but not by co-formation. With this method, the distribution of the

dopant element in LDH takes place on the surface. Unlike anionic dye, the cationic dye cannot intercalate into LDH, so its sorption happened on the surface and photodegradation increased due to surface defects. Defects that were more formed during Ag doping and had a high distribution on the surface. The maximal adsorption degree is observed by Cu and Cd doping metals (Table 1) for anionic dye because of the increasing of positive charges. In contrast to adsorption, the photodegradation degree of as-obtained undoped ZnAl-LDH/PVA nanocomposite is high for anionic dye (P4R) (Figure 3), but it is enhanced by Cd, Fe, Ag, Co, Sr and Ca dopants. The maximal photodegradation degree is observed by Sr and Fe doping metals. In spite of the fact that Cu-doped LDH shows high adsorption, the photodegradation degree is happened very low (~60%). In the literature, the increase of photocatalytic activity with doping is mainly explained by the decrease of the band gap energy and thus the increase of the electron transition [44]. The results of the research work are consistent with this concept. So the band gap energy decreased from 3.12 eV to 3.1 eV by Sr and Ag, 3.09 eV by Pb, 3.08 eV by Cd, 3.06 eV by Co, 3 eV by Cu and Ni, 2.6 eV by Fe and 2.2 eV by La dopants (Figure 4). However, the nature of the dopants, whether they are s, d or f elements, and thus the formation of n- or p-type conductivity directly affects the recombination of h⁺ and e⁻ pairs, as well as the decomposition of dyes by the resulting radicals.

**SYNTHESIS OF DIFFERENT METAL DOPED ZnAl-LDH/PVA NANOCOMPOSITES
FOR ADSORPTION AND PHOTOCATALYTIC APPLICATIONS**

Table 1. Adsorption and photocatalytic degradation degrees of P4R anionic dye onto as-obtained and metal doped ZnAl-LDH/PVA nanocomposites

Doping metals	—	Cd	Cu	Fe	Ag	Co	Ni	Sr	Ca	Pb
Sorption degree,%	50.98	64.40	66.54	54.92	43.47	54.74	55.99	45.97	51.87	41.68
Photodegradation degree,%	92.07	94.09	60.08	94.90	93.10	93.48	89.00	95.32	92.26	91.04

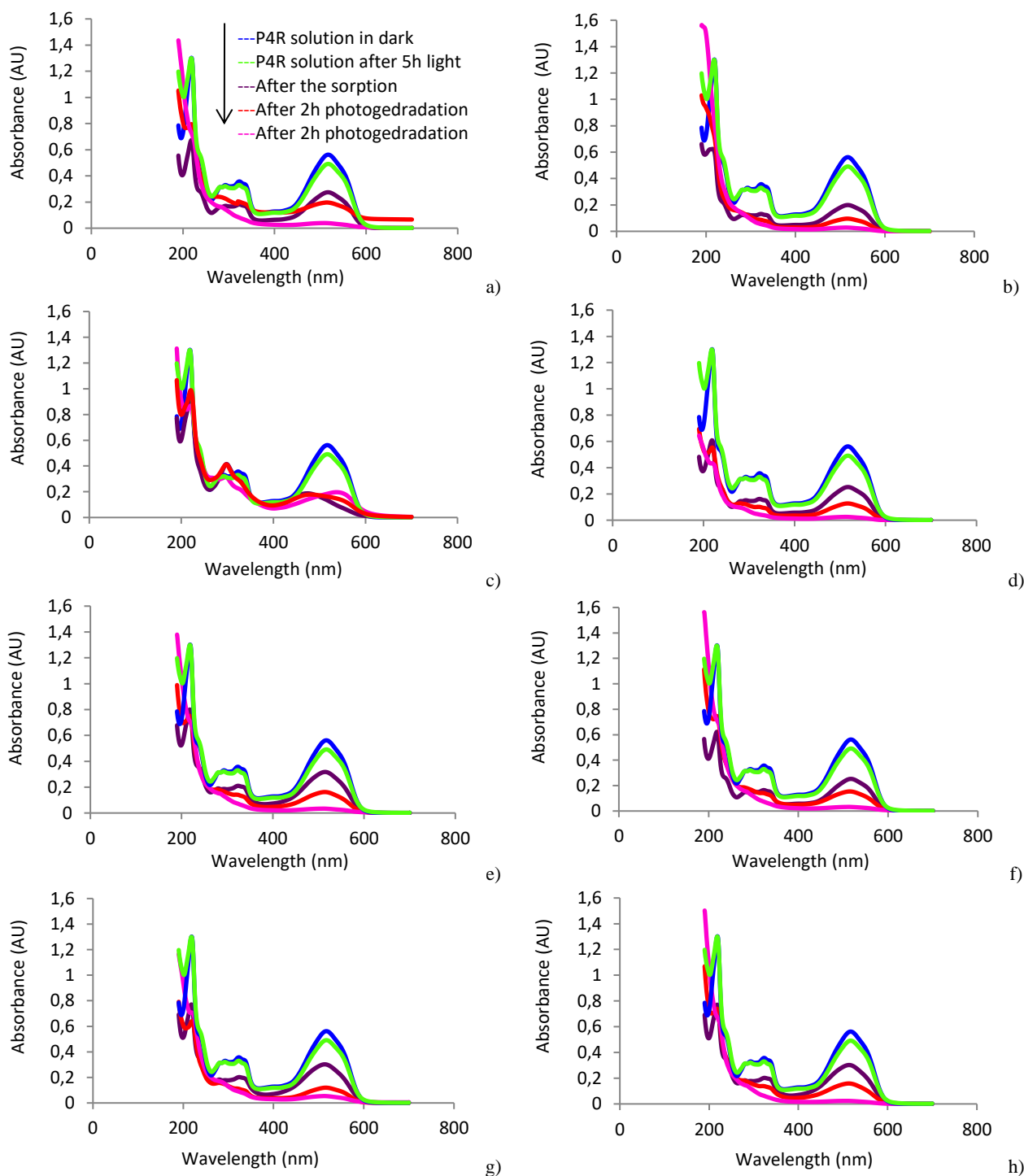


Figure 3. Adsorption and photocatalytic degradation of P4R anionic dye onto as-obtained (a) and Cd (b), Cu (c), Fe (d), Ag (e), Co (f), Ni (g), Sr (h), Ca (i) and Pb (j) – doped ZnAl-LDH/PVA nanocomposites

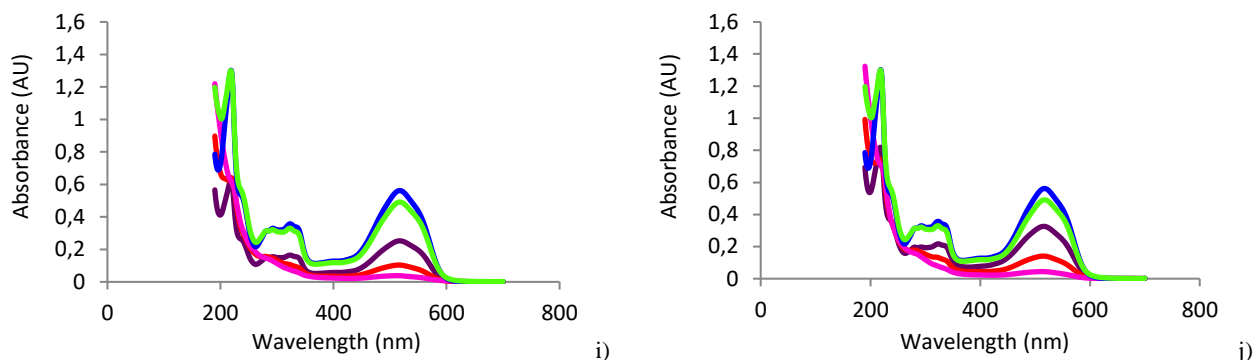


Figure 3 (continued). Adsorption and photocatalytic degradation of P4R anionic dye onto as-obtained (a) and Cd (b), Cu (c), Fe (d), Ag (e), Co (f), Ni (g), Sr (h), Ca (i) and Pb (j) – doped ZnAl-LDH/PVA nanocomposites

Table 2. Adsorption and photocatalytic degradation degrees of R6G anionic dye onto as-obtained and metal doped ZnAl-LDH/PVA nanocomposites.

Doping metals	As obtained	—	Cd	Cu	Fe	Ag	La	Ni	Sr	Ca	Pb
Sorption degree,%	19.59	31.05	23.51	16.45	10.68	19.00	5.78	10.97	17.43	16.93	10.58
Photodegradation degree,%	88.54	87.56	79.43	66.01	57.98	81.78	67.87	66.11	81.39	75.51	65.13

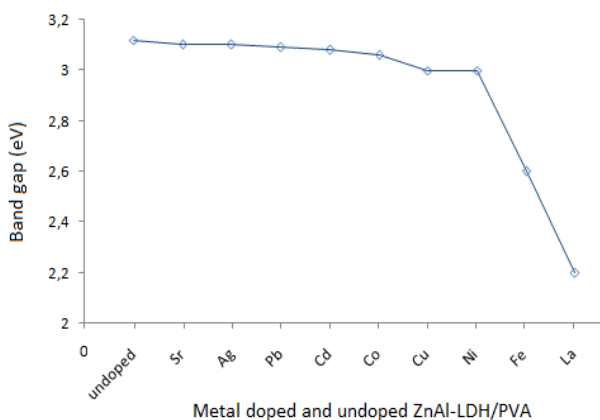


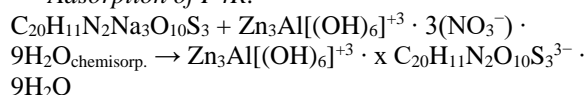
Figure 4. Band gap values of metal doped and undoped ZnAl-LDH/PVA nanocomposite

As can be seen from Table 2, pure ZnAl-LDH/PVA nanocomposites without any doping are an excellent photocatalyst for cationic dye (R6G). The effectivity increased from adsorption to photodegradation (Figure 5). Here La did not affect the adsorption, in contrast the sorption degree occurred very low. The potential effectiveness of using rare-earth elements-LDHs and their related oxides as photocatalysts are being investigated by numerous authors [45]. The authors confirm that, the co-existence of La³⁺ species leads to an improvement in the photocatalytic properties of LDH materials [40, 46]. Here the photocatalytic degradation activity of R6G increased despite very low adsorption and reached to 67.87% which is also not a good result beside undoped- and Sr, Ag, Cd and Ca doped LDH. It can be released the electrostatic repulsion interaction between these elements and cationic dye. As a result, we can say that, both adsorption and photocatalytic degradation of cationic dye like R6G is better with undoped ZnAl-LDH/PVA nanocomposite

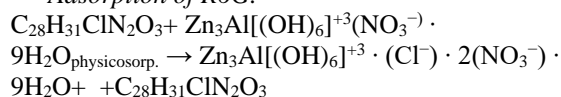
than the metal doped ones. As can be seen from the Figure 5, b, h and i, the intensity of absorbance bands at low wavelength decreased significantly which are correspond to organic and aromatic species. As can be seen from the spectra, if the photocatalyst is not used, the photodegradation of dyes also takes place with low degree (Figures 1, 2). The decomposition of R6G without catalyst is faster than that of P4R. In Cd-doped LDH, the light decomposition curve without catalyst almost overlaps the sorption curve.

The photocatalytic degradation mechanism can be described as follow [47-53]:

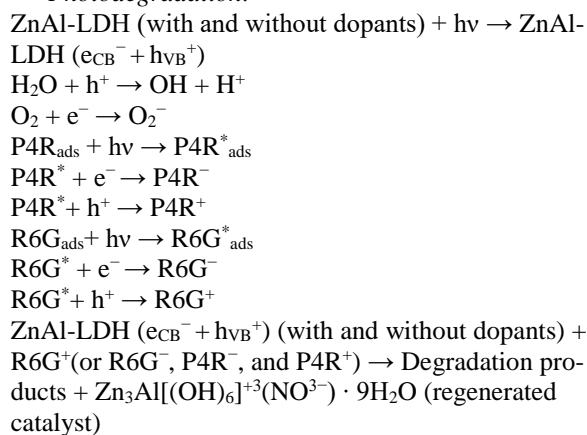
Adsorption of P4R:



Adsorption of R6G:



Photodegradation:



**SYNTHESIS OF DIFFERENT METAL DOPED ZnAl-LDH/PVA NANOCOMPOSITES
FOR ADSORPTION AND PHOTOCATALYTIC APPLICATIONS**

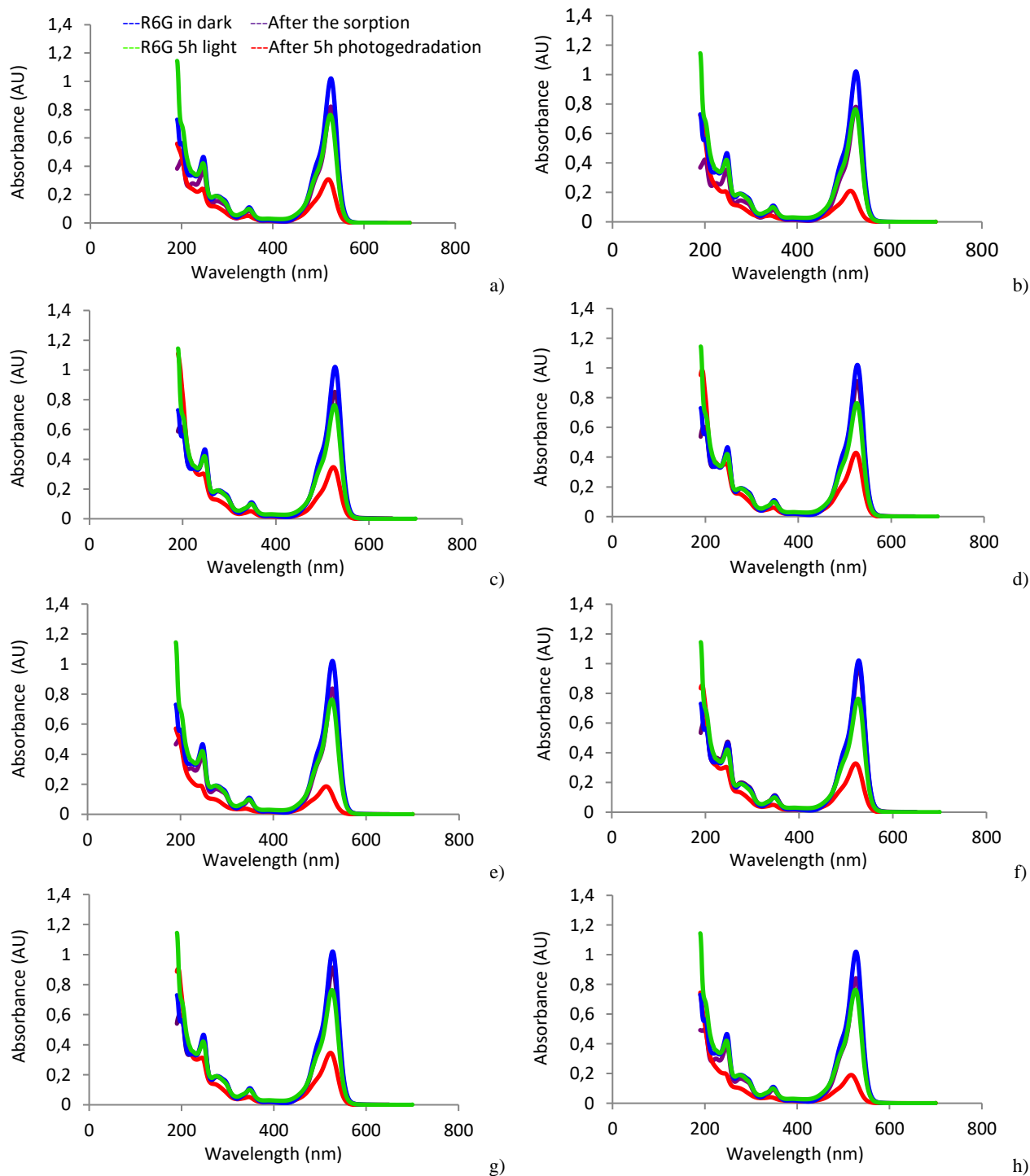


Figure 5. Adsorption and photocatalytic degradation of R6G cationic dye onto as-obtained (a) and Cd (b), Cu (c), Fe (d), Ag (e), La (f), Ni (g), Sr (h), Ca (i) and Pb (j) – doped ZnAl-LDH/PVA nanocomposites.

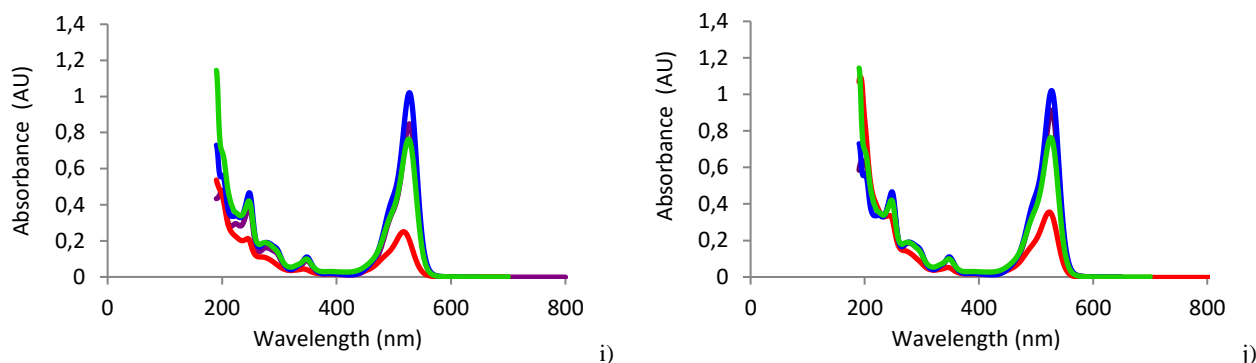


Figure 5 (continued). Adsorption and photocatalytic degradation of R6G cationic dye onto as-obtained (a) and Cd (b), Cu (c), Fe (d), Ag (e), La (f), Ni (g), Sr (h), Ca (i) and Pb (j) – doped ZnAl-LDH/PVA nanocomposites

4. CONCLUSIONS

The synthesis of ZnAl-LDH/PVA nanocomposite and its doping with various metals by impregnation method were discussed in this research article. The influence of dopant element to the sorption and photodegradation is also studied. Because the P4R is an anionic dye, it intercalated the layered structure by expanding the basal distance from 0.7 nm to 0.762 nm, but the cationic dye (R6G) could not. The doubling of diffraction peaks corresponding 003 Miller index is explained by the formation of two phases (relaxed and strained) under the light. It turned out that the photodegradation improved by the metal doping of LDH for anionic dye and weakened for cationic dye because of the electrostatic interaction between the dyes molecules and layered structure.

REFERENCES

- Saleh T.A. Nanomaterials: Classification, properties, and environmental toxicities // *Environmental Technology & Innovation*. – 2020. – Vol 20:101067. <https://doi.org/10.1016/j.eti.2020.101067>
- Liu Z., Navik R., Tan H., et al. Graphene-based materials prepared by supercritical fluid technology and its application in energy storage // *The Journal of Supercritical Fluids*. – 2022. – Vol. 188:105672. <https://doi.org/10.1016/j.supflu.2022.105672>
- Mirzaei A., Oum W., Ham H., et al. Catalyst and substrate-free synthesis of graphene nanosheets by unzipping C₆₀ fullerene clusters using a pulse current method // *Materials Science in Semiconductor Processing*. – 2022. – Vol. 149:106831. <https://doi.org/10.1016/j.mssp.2022.106831>
- Isseroff R., Blackburn L., Chen A., et al. (2016) Synthesis and Characterization of Partially Reduced Graphene Oxide and Platinum and Gold Partially Reduced Graphene Oxide // *MRS Advances*. – 2016. – Vol. 1. – PP. 1345–1351. <https://doi.org/10.1557/adv.2016.89>
- Zhou H., Jiresse N.K.L., Zhang W., et al. MXene-derived TiO₂/MXene-loaded Ag for the degradation of the methyl orange // *Journal of Materials Research*. – 2021. – Vol. 36. – PP. 5002–5012. <https://doi.org/10.1557/s43578-021-00428-7>
- Preschilla N., Rasheed A.S.A., Sahadevan S., et al. (2010) Study of layered silicate clays as synergistic nucleating agent for polypropylene // *Journal of Polymer Science Part B: Polymer Physics*. – 2010. – Vol. 48. – PP. 1786–1794. <https://doi.org/10.1002/polb.22044>
- Jaiswal A., Gautam R.K., Chattopadhyaya M.C. Layered Double Hydroxides and the Environment: An Overview // *Advanced Materials for Agriculture, Food, and Environmental Safety*. – 2014. – Vol. 9781118773437. – PP. 1–26. <https://doi.org/10.1002/9781118773857.ch1>
- Jiang J.Q., Ashekuzaman S.M. Preparation and evaluation of layered double hydroxides (LDHs) for phosphate removal // *Desalination and Water Treatment*. – 2015. – Vol. 55. – PP. 836–843. <https://doi.org/10.1080/19443994.2014.934734>
- Zhang H., Balaji Y., Nalin Mehta A., et al. (2018) Formation mechanism of 2D SnS₂ and SnS by chemical vapor deposition using SnCl₄ and H₂S // *Journal of Materials Chemistry C*. – 2018. Vol. 6. – PP. 6172–6178. <https://doi.org/10.1039/c8tc01821a>
- Li X., Zhu H. Two-dimensional MoS₂: Properties, preparation, and applications // *Journal of Materiomics*. – 2015. – Vol. 1. – PP. 33–44. <https://doi.org/10.1016/j.jmat.2015.03.003>
- Lashgari H., Boochani A., Shekaari A., et al. (2016) Electronic and optical properties of 2D graphene-like ZnS: DFT calculations // *Applied Surface Science*. – 2016. – Vol. 369. – PP. 76–81. <https://doi.org/10.1016/j.apsusc.2016.02.042>
- Zhao Y., Liu N., Zhou S., Zhao J. (2019) Two-dimensional ZnO for the selective photoreduction of CO₂ // *Journal of Materials Chemistry A*. – 2019. – Vol. 7. – PP. 16294–16303. <https://doi.org/10.1039/c9ta04477a>
- Wang G., Zhi Y., Xia L., et al. 2D CdO-Based Heterostructure as a Promising Visible Light Water-Splitting Photocatalyst // *Physica Status Solidi (A) Applications and Materials Science*. – 2020. – Vol. 217:1900859. <https://doi.org/10.1002/pssa.201900859>
- Ji J., Song X., Liu J., et al. Two-dimensional antimonene single crystals grown by van der Waals epitaxy // *Nature Communications*. – 2016. – Vol. 7:13352. <https://doi.org/10.1038/ncomms13352>
- Nicolosi V., Chhowalla M., Kanatzidis M.G., et al. Liquid exfoliation of layered materials // *Science*. – 2013. – Vol. 340, Issue. 6139. – P. 1226419. <https://doi.org/10.1126/science.1226419>

16. Hu T., Mei X., Wang Y., et al. Two-dimensional nano-materials: fascinating materials in biomedical field // *Science Bulletin*. – 2019. – Vol. 64. – PP. 1707–1727. <https://doi.org/10.1016/j.scib.2019.09.021>
17. Yang B., Cai J., Wei S., et al. Preparation of Chitosan/NiFe-layered double hydroxides composites and its fenton-like catalytic oxidation of phenolic compounds // *Journal of Polymers and the Environment*. – 2020. – Vol. 28. – PP. 343–353. <https://doi.org/10.1007/s10924-019-01614-9>
18. Mohapatra L., Parida K., Satpathy M. Molybdate/tungstate intercalated oxo-bridged Zn/Y LDH for solar light induced photodegradation of organic pollutants // *The Journal of Physical Chemistry C*. – 2012. – Vol. 116. – PP. 13063–13070. <https://doi.org/10.1021/jp300066g>
19. Xia S., Qian M., Zhou X., et al. Theoretical and experimental investigation into the photocatalytic degradation of hexachlorobenzene by ZnCr layered double hydroxides with different anions // *Molecular Catalysis*. – 2017. – Vol. 435. – PP. 118–127. <https://doi.org/10.1016/j.mcat.2017.03.024>
20. Chen Y., Ouyang Y., Yang J., et al. Facile Preparation and Performances of Ni, Co, and Al Layered Double Hydroxides for Application in High-Performance Asymmetric Supercapacitors // *ACS Applied Energy Materials*. – 2021. – Vol. 4, Issue. 9. – PP. 9384–9392. <https://doi.org/10.1021/acsaem.1c01575>
21. Li X., Du D., Zhang Y., et al. Layered double hydroxides toward high-performance supercapacitors // *Journal of Materials Chemistry A*. – 2017. Vol. 5. – PP. 15460–15485. <https://doi.org/10.1039/c7ta04001f>
22. Babu H.V., Coluccini C., Wang D-Y. Functional layered double hydroxides and their use in fire-retardant polymeric materials // *Novel Fire Retardant Polymers and Composite Materials*. – 2017. PP. 201–238. <https://doi.org/10.1016/b978-0-08-100136-3.00008-x>
23. Zhu K., Wang Y., Tang D., et al. Flame-retardant mechanism of layered double hydroxides in asphalt binder / *Materials (Basel)*. – 2019. – Vol. 12(5):801. <https://doi.org/10.3390/MA12050801>
24. Dou Y., Pan T., Zhou A., et al. (2013) Reversible thermally-responsive electrochemical energy storage based on smart LDH@P(NIPAM-co-SPMA) films / *Chemical Communications*. – 2013. – Vol. 49. – PP. 8462–8464. <https://doi.org/10.1039/c3cc43039a>
25. Das A.K., Pan U.N., Sharma V., et al. Nanostructured CeO₂/NiV-LDH composite for energy storage in asymmetric supercapacitor and as methanol oxidation electrocatalyst / *Chemical Engineering Journal*. – 2021. – Vol. 417:128019. <https://doi.org/10.1016/j.cej.2020.128019>
26. Costantino U., Vivani R., Bastianini M., et al. Ion exchange and intercalation properties of layered double hydroxides towards halide anions / *Dalton Transactions*. – 2014. – Vol. 43. – P. 11587–11596. <https://doi.org/10.1039/c4dt00620h>
27. Zou W., Guo W., Liu X., et al. Anion Exchange of Ni-Co Layered Double Hydroxide (LDH) Nanoarrays for a High-Capacitance Supercapacitor Electrode: A Comparison of Alkali Anion Exchange and Sulfuration // *Chemistry – A European Journal*. – 2018. – Vol. 24. – P. 19309–19316. <https://doi.org/10.1002/chem.201804218>
28. Jin W., Park D.H. Functional layered double hydroxide nanohybrids for biomedical imaging // *Nanomaterials*. – 2019. – Vol. 9(10):1404. <https://doi.org/10.3390/nano9101404>
29. Yan L., Gonca S., Zhu G., et al. Layered double hydroxide nanostructures and nanocomposites for biomedical applications // *Journal of Materials Chemistry B*. – 2019. – Vol. 7. – PP. 5583–5601. <https://doi.org/10.1039/c9tb01312a>
30. Baig N., Sajid M. Applications of layered double hydroxides based electrochemical sensors for determination of environmental pollutants: A review // *Trends in Environmental Analytical Chemistry*. – 2017. Vol. 16. – PP. 1–15. <https://doi.org/10.1016/j.teac.2017.10.003>
31. Zhao Q., Wang M., Yang H., Shi D., Wang Y. Preparation, characterization and the antimicrobial properties of metal ion-doped TiO₂ nano-powders // *Ceramics International*. – 2018. Vol. 44(5). PP. 5145–5154.
32. Guayaquil-Sosa J.F., Serrano-Rosales B., Valadés-Pelayo P.J., de Lasa H. Photocatalytic hydrogen production using mesoporous TiO₂ doped with Pt // *Applied Catalysis B: Environmental*. – 2017. – Vol. 211. – PP. 337–348.
33. Balayeva O.O. Synthesis and characterization of zinc-aluminum based layered double hydroxide and oxide nanomaterials by performing different experimental parameters // *Journal of Dispersion Science and Technology*. – 2022. – Vol. 43. – PP. 1187–1196. <https://doi.org/10.1080/01932691.2020.1848580>
34. Chuaicham C, Xiong Y, Sekar K, et al. A promising Zn-Ti layered double hydroxide/Fe-bearing montmorillonite composite as an efficient photocatalyst for Cr(VI) reduction: Insight into the role of Fe impurity in montmorillonite // *Applied Surface Science*. – 2021. – Vol. 546: 148835. <https://doi.org/10.1016/j.apsusc.2020.148835>
35. Sayler RI, Hunter BM, Fu W, et al. EPR Spectroscopy of Iron- and Nickel-Doped [ZnAl]-Layered Double Hydroxides: Modeling Active Sites in Heterogeneous Water Oxidation Catalysts // *Journal of the American Chemical Society*. – 2020. – Vol. 142. PP. 1838–1845. <https://doi.org/10.1021/jacs.9b10273>
36. Morales-Mendoza G, Tzompantzi F, García-Mendoza C, et al. (2015) Mn-doped Zn/Al layered double hydroxides as photocatalysts for the 4-chlorophenol photodegradation // *Applied Clay Science*. – 2015. – Vol. 118. – PP. 38–47. <https://doi.org/10.1016/j.clay.2015.08.030>
37. Zhang Y., Liu J., Li Y., et al. Enhancement of active anticorrosion via Ce-doped Zn-Al layered double hydroxides embedded in sol-gel coatings on aluminum alloy // *The Journal of Wuhan University of Technology-Mater. Sci. Ed.* – 2017. – Vol. 32. – PP. 1199–1204. <https://doi.org/10.1007/s11595-017-1731-6>
38. Fu Y., Ning F., Xu S., et al. Terbium doped ZnCr-layered double hydroxides with largely enhanced visible light photocatalytic performance // *Journal of Materials Chemistry A*. – 2016. – Vol. 4. – PP. 3907–3913. <https://doi.org/10.1039/c5ta10093c>
39. Wen R., Yang Z., Chen H., et al. Zn-Al-La hydrotalcite-like compounds as heating stabilizer in PVC resin // *Journal of Rare Earths*. – 2012. – Vol. 30. – PP. 895–902. [https://doi.org/10.1016/S1002-0721\(12\)60151-3](https://doi.org/10.1016/S1002-0721(12)60151-3)
40. Dinari M., Momeni M.M., Ghayeb Y. Photodegradation of organic dye by ZnCrLa-layered double hydroxide as visible-light photocatalysts // *Journal of Materials Science: Materials in Electronics*. – 2016. – Vol. 27. – PP. 9861–9869. <https://doi.org/10.1007/s10854-016-5054-8>

41. Kappertz O., Drese R., Wuttig M. Correlation between Structure, Stress and Deposition Parameters in Direct Current Sputtered Zinc Oxide Films // *Journal of Vacuum Science & Technology A*. – 2002. – Vol. 20:2084. <https://doi.org/10.1116/1.1517997>
42. Banerjee, S.; Chattopadhyaya, M. C. Adsorption Characteristics for the Removal of a Toxic Dye.; Tartrazine from Aqueous Solutions by a Low Cost Agricultural by-Product // *Arabian Journal of Chemistry*. – 2017. – Vol. 10(2). – PP. S1629–S1638. <https://doi.org/10.1016/j.arabjc.2013.06.005>
43. Balayeva O.O., Azizov A.A., Muradov M.B., Alosmanov R.M. Removal of tartrazine, ponceau 4R and patent blue V hazardous food dyes from aqueous solutions with ZnAl-LDH/PVA nanocomposite // *Journal of Dispersion Science and Technology*. – 2021. – PP. 1–14. <https://doi.org/10.1080/01932691.2021.2006688>
44. Liu Sh., Min Z., Hu D., Liu Y. Synthesis of calcium doped TiO₂ nanomaterials and their visible light degradation property. International Conference on Material and Environmental Engineering (ICMAEE 2014). <https://doi.org/10.2991/icmaee-14.2014.12>
45. Seliverstov E.S., Golovin S.N., Lebedeva O.E. (2022) Layered Double Hydroxides Containing Rare Earth Cations: Synthesis and Applications // *Frontiers in Chemical Engineering*. – 2022. – Vol. 4. <https://doi.org/10.3389/fceng.2022.867615>
46. Gao L.G., Li H.X., Song X.L., et al. Degradation of benzothiophene in diesel oil by LaZnAl layered double hydroxide: photocatalytic performance and mechanism // *Petroleum Science*. – 2019. Vol. 16. – PP. 173–179. <https://doi.org/10.1007/s12182-018-0285-3>
47. Balayeva O.O. Photocatalytic degradation of Ponceau 4R by ZnAl-layered double hydroxide nanostructures obtained with and without polyvinyl alcohol // *Journal of the Chinese Chemical Society*. – 2022. – Vol. 69, Issue 9. – PP. 1594–1607. <https://doi.org/10.1002/jccs.202200121>
48. Bouarroudj T., Aoudjit L., Djahida L., Zaidi B., Ouraghi M., Zioui D., Mahidine S., Shekhar C. and Bachari K. Photodegradation of tartrazine dye favored by natural sunlight on pure and (Ce, Ag) co-doped ZnO catalysts // *Water Science & Technology*. – 2021. – Vol. 83, Issue 9. – PP. 2118–2134. <https://doi.org/10.2166/wst.2021.106>
49. Chen Y., Yang S., Wang K., Lou L. Role of primary active species and TiO₂ surface characteristic in UV-illuminated photodegradation of Acid Orange 7 // *Journal of Photochemistry and Photobiology A: Chemistry*. – 2005. – Vol. 172. PP. 47–54. <https://doi.org/10.1016/j.jphotochem.2004.11.006>
50. Fujishima A., Zhang X., Tryk D., TiO₂ photocatalysis and related surface phenomena // *Surface Science Reports*. – 2008. – Vol. 63. – PP. 515–582. <https://doi.org/10.1016/j.surfrep.2008.10.001>
51. Kumaran N.N., Muraleedharan K. Photocatalytic activity of ZnO and Sr²⁺ doped ZnO nanoparticles // *Journal of Water Process Engineering*. – 2017. – Vol. 17. – PP. 264–270. <https://doi.org/10.1016/j.jwpe.2017.04.014>
52. Ani I.J., Akpan U.G., Olutoye M.A., Hameed B.H. Photocatalytic degradation of pollutants in petroleum refinery wastewater by TiO₂- and ZnO-based photocatalysts: Recent development // *Journal of Cleaner Production*. – 2018. – Vol. 205. – PP. 930–954. <https://doi.org/10.1016/j.jclepro.2018.08.189>
53. Lin Y.Y., Chi H.T., Lin J.H., Chen F.H., Chen C.C., Lu C.S. Eight crystalline phases of bismuth vanadate by controllable hydrothermal synthesis exhibiting visible-light-driven photocatalytic activity // *Molecular Catalysis*. – 2021. – Vol. 506:111547. <https://doi.org/10.1016/j.mcat.2021.111547>

МЕТАЛЛ ЛЕГИРЛЕНГЕН ZnAl- ҚҚГ / ПВС НАНОКОМПОЗИТТЕРІ: СИНТЕЗ ЖӘНЕ СОРБЦИЯЛЫҚ-ФОТОКАТАЛИТИКАЛЫҚ ҚОЛДАНУ

О.О. Балаева

Баку мемлекеттік университеті, Баку, Әзірбайжан

Екі өлшемді нанокұрылымдар (2D) жоғары бетінің ауданына, электронды қасиеттеріне, энергия сақтау өнімділігіне және каталитикалық белсенділігіне байланысты ғылымды дамытуда үлкен қызығушылық пен үлкен назар аударды. Қабатты қосарланған гидроксидтер (ҚҚГ) 2D нанокұрылымдарына жатады және жоғары беттік ауданы, өте маңызды физика-химиялық қасиеттері және биологиялық белсенділігі бар. Дегенмен, осы бірегей қасиеттерді, әсіресе фотокаталитикалық белсенділікті жақсарту және жақсарту үшін олардың допингіне әрқашан үлкен қызығушылық болды. Бұл жұмыста ZnAl негізіндегі LDH синтезделді және олардың белсенді- (Ca, Sr), ауысу- (Co, Cu, Cd, Ni, Pb, Fe), асыл- (Ag) және сирек жер- (La) металдар сіңдіру әдісімен жүргізілді. Синтезделген және легирленген ZnAl-ҚҚГ/поливинил спирті нанокөмірдің адсорбция және фотодеградация арқылы сулы ерітінділерден катиондық және анионды бояғыштарды жою да зерттелді. Алынған нәтижелер нанокөмірдің құрылымымен және физика-химиялық қасиеттерімен корреляцияланды.

Түйін сөздер: *Қабатты қос гидроксидтер (ҚҚГ), металл қоспасы, сорбция, фотодеградация, Родамин 6G, Понсо 4R.*

СИНТЕЗ И СОРБЦИОННО-ФОТОКАТАЛИТИЧЕСКОЕ ПРИМЕНЕНИЕ ЛЕГИРОВАННЫХ
МЕТАЛЛАМИ НАНОКОМПОЗИТОВ ZnAl- СДГ/ПВС

О.О. Балаева

Бакинский государственный университет, Баку, Азербайджан

Двумерные наноструктуры (2D) привлекли значительный интерес и большое внимание в современной науке, благодаря своей большой площади поверхности, электронным свойствам, характеристикам накопления энергии и каталитической активности. Слоистые двойные гидроксиды (СДГ) относятся к двумерным наноструктурам и обладают большой площадью поверхности, очень важными физико-химическими свойствами и биологической активностью. Однако всегда существовал большой интерес к их легированию для усиления и улучшения этих свойств, особенно фотокаталитической активностью. В данной работе были синтезированы СДГ на основе ZnAl и проведено их легирование активными (Ca, Sr), переходными (Co, Cu, Cd, Ni, Pb, Fe), благородными (Ag) и редкоземельными элементами (La) осуществлялись методом пропитки. Также было изучено удаление катионных и анионных красителей из водных растворов путем адсорбции и фотодегградации на свежесинтезированном и легированном нанокompозите ZnAl-СДГ/ПВС. Полученные результаты сопоставлены со структурой и физико-химическими свойствами нанокompозитов.

Ключевые слова: Слоистые двойные гидроксиды (СДГ), легированные металлами, сорбция, фотодегградация, Родамин 6G, Понсо 4R.